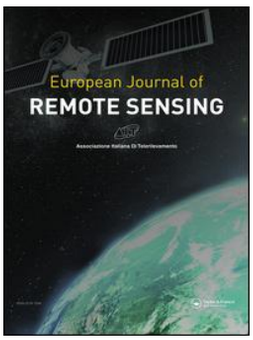

European Journal of Remote Sensing

ISSN: (Print) 2279-7254 (Online) Journal homepage: http://www.tandfonline.com/loi/tejr20

Laser Scanning Application for Geostructural analysis of Tuffaceous Coastal Cliffs: the case of Punta Epitaffio, Pozzuoli Bay, Italy

Fabio Matano, Antonio Pignalosa, Ermanno Marino, Giuseppe Esposito, Mauro Caccavale, Teresa Caputo, Marco Sacchi, Renato Somma, Claudia Troise & Giuseppe De Natale

To cite this article: Fabio Matano, Antonio Pignalosa, Ermanno Marino, Giuseppe Esposito, Mauro Caccavale, Teresa Caputo, Marco Sacchi, Renato Somma, Claudia Troise & Giuseppe De Natale (2015) Laser Scanning Application for Geostructural analysis of Tuffaceous Coastal Cliffs: the case of Punta Epitaffio, Pozzuoli Bay, Italy, European Journal of Remote Sensing, 48:1, 615-637, DOI: 10.5721/EuJRS20154834

To link to this article: https://doi.org/10.5721/EuJRS20154834

Published online: 17 Feb 2017.

European Journal of Remote Sensing - 2015, 48: 615-637
doi: 10.5721/EuJRS20154834
Received 04/11/2014, accepted 22/06/2015

European Journal of Remote Sensing
An official journal of the Italian Society of Remote Sensing

www.aitjournal.com

Laser Scanning Application for Geostructural analysis of Tuffaceous Coastal Cliffs: the case of Punta Epitaffio, Pozzuoli Bay, Italy

Fabio Matano[1]*, Antonio Pignalosa[2], Ermanno Marino[2], Giuseppe Esposito[1], Mauro Caccavale[1], Teresa Caputo[3], Marco Sacchi[1], Renato Somma[3], Claudia Troise[3] and Giuseppe De Natale[3]

[1]Consiglio Nazionale delle Ricerche (CNR), Istituto per l'Ambiente Marino Costiero, Calata Porta di Massa, Porto di Napoli, 80133, Napoli, Italy
[2]Stage srl, Viale Gandhi 72, 81025, Marcianise (Caserta), Italy
[3]Istituto Nazionale di Geofisica e Vulcanologia, Sezione di Napoli, Osservatorio Vesuviano, Via Diocleziano 328, 80124, Napoli, Italy
*Corresponding author, e-mail address: fabio.matano@cnr.it

Abstract

This study presents the results of a Terrestrial Laser Scanner (TLS) application aimed at characterizing the structural pattern of Punta Epitaffio tuffaceous coastal cliff, Pozzuoli Bay, Eastern Tyrrhenian margin. The study site is located in the Campi Flegrei, an active volcanic caldera, characterized by dense urbanization, near the town of Naples, Italy. The 3D digital model of the Punta Epitaffio cliff derived from TLS data, provided a base for the classification of rock discontinuities by geostatistical analysis. In particular, the work flow of geostructural data processing included: 1) statistical analysis of spatial orientation of the facets of the 3D mesh derived by the TLS survey; 2) extraction of the best-fit attitudes (dip and dip direction) of discontinuity sets for each sub-planar patch of the rock face; 3) cluster analysis of best-fit structural discontinuities; 4) definition of all the discontinuity sets and geo-structural classification of 3D model facets; 5) kinematic analysis for the definition of possible failure mechanisms. Kinematic analysis took into account primarily structurally-controlled failure mechanisms (planar sliding, wedge sliding, flexural toppling, and direct toppling). The method illustrated in this research can be extensively applied to identify unstable areas along tuffaceous coastal cliffs and define shape and volume of rocks potentially involved by failures.

Keywords: Tuff cliff, joint sets, rock failures, terrestrial laser scanning, Punta Epitaffio, Italy.

Introduction

Coastal cliffs are characterized by relatively rapid morphological evolution due to intense erosion, accompanied by failure processes, at the sea-land interface. The rates of erosion and retreat may be enhanced in cliffed coasts formed by pyroclastic deposits and tuffs produced by explosive volcanism. In this case frequent jointing of welded tuff outcrops

due to thermal and/or volcano-tectonic effects, along with the relatively low competence of many volcaniclastic deposits, results in accelerated marine weathering of rock slopes.

In recent years, Terrestrial Laser Scanner (TLS) has been increasingly applied for ground surface surveying and monitoring as well as geohazard assessment with specific reference to slope instability, landslides and lava flow in coastal volcanic areas [Hunter et al., 2003; Bitelli et al., 2004; Barbarella and Fiani, 2013; Abellán et al., 2014]. Particularly interesting is the application of TLS technique for the high-resolution monitoring of landslide phenomena on rocky coast [Olsen et al., 2009; Lim et al., 2010; Young et al., 2011; Abellan et al., 2014; Matano et al., 2015]. In the cliff sectors, rock discontinuities can play an important role in controlling the failure mechanism and represent a key factor to evaluate the susceptibility of slopes to block failures. In light of the above, in this research we developed a long-range TLS application addressed to the geostructural analysis of some segments of the tuff coastal cliff facing the eastern sector of the Pozzuoli Bay, located ca. 10 km to the west of the town of Naples, southern Italy.

The Pozzuoli Bay represents the offshore counterpart of the Campi Flegrei caldera [Sacchi et al., 2014], an active volcanic district characterized by intense explosive activity during the latest Quaternary and dramatic ground deformation caused by bradyseismic phenomena [Del Gaudio et al., 2010]. The Campi Flegrei caldera has a quasi-circular shape with a radius of ca. 12 km and is a highly urbanized sector of the Campania coastal zone, characterised by a population of more than 300,000 inhabitants and relevant infrastructures, thus representing one of the highest volcanic risk areas in the world [De Natale et al., 2006]. In addition to volcanic eruptions, the whole area is prone to a series of natural and anthropogenic hazards, including earthquakes, tsunamis, ground deformation, floods, storm surges, landslides and coastal erosion [Beneduce et al., 1988; Lirer et al., 2001].

The coastal zone of the Pozzuoli Bay is formed by rocky cliffs with subordinate sandy beach segments. Cliffs mostly consist of welded to partly welded tuffs and ignimbrites and coherent to loose volcaniclastic deposits. The tuffaceous cliffs are characterized by rapid geomorphological evolution due to intense fracturing, weathering and failure processes, including mechanisms classified as rock fall, rock topple and rock slide. Instability processes are favoured by several factors, such as the occurrence of a complex network of structural discontinuities, and the juxtaposition of different rock types characterized by extremely variable cohesion, cementation grade, and differential erosion [Evangelista et al., 2010].

A number of sites particularly exposed to the risk of failure have been selected on the basis of an inventory of the coastal tuffaceous cliffs of the Pozzuoli bay. These sites (Fig. 1) are the focus of current surveying and monitoring activities within the frame of the research project “MONICA” dedicated to hazard mitigation and realization of a prototype of an early warning system for the Pozzuoli Bay area on the basis of innovative integrated technology including optic fiber devices and networks [Esposito et al., 2013; Matano et al., 2014; Somma et al., 2014; Matano et al., 2015].

This paper presents the results of a geostructural analysis of the Punta Epitaffio tuff cliff test site (Fig. 1). The procedure, already adopted for the study of Coroglio tuff cliff [Matano et al., 2015], is based on a workflow that includes TLS data acquisition and processing, 3D model development, geostructural data classification, failure kinematic analysis. All data have been managed with a Geographical Information System (GIS). The main purpose of this study is the TLS-based analysis of the discontinuity sets that characterize the Punta

Epitaffio cliff, addressed to the understanding of the possible failure mechanisms. These geostructural data are necessary for the mapping of unstable areas along the cliffs, and the estimation of the rock volumes potentially involved by landslides phenomena.
TLS based monitoring of the tuffaceous cliffs of the Pozzuoli Bay is of primary interest for the understanding of morphogenetic processes associated with the evolution of the coastal zone and provides the necessary integration to Civil Protection authorities for the assessment of the full spectrum of natural hazards in a volcanically active area.

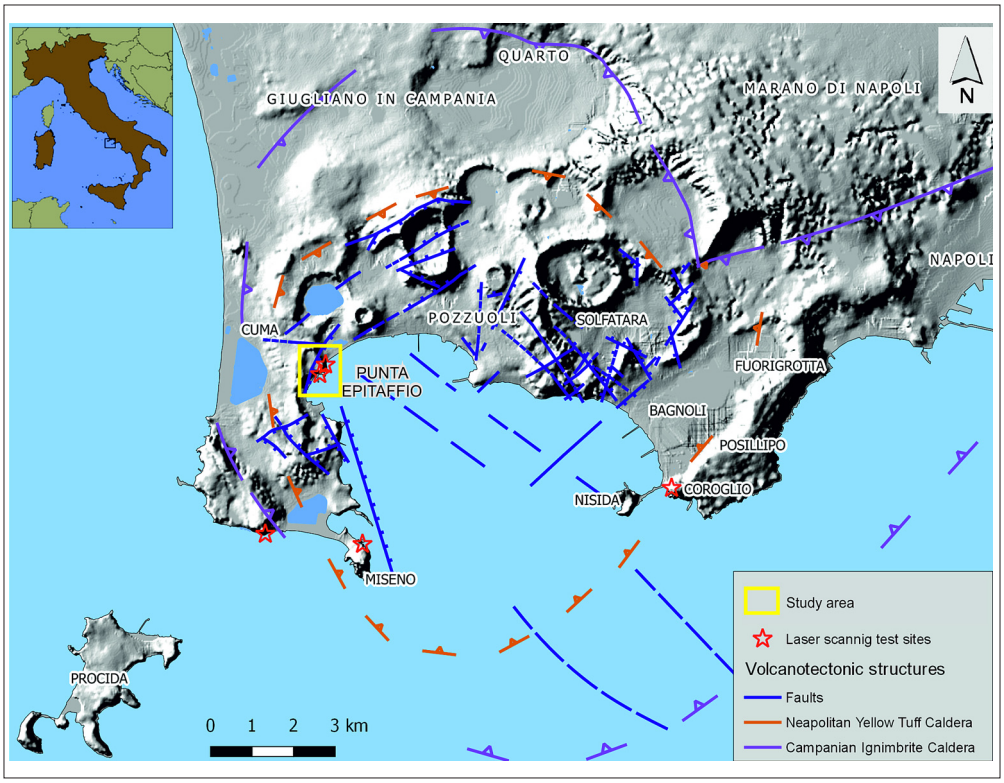

Figure 1 - Study area with main volcano-tectonic structures [Orsi et al., 1996] and location of selected tuff cliffs. The hillshade derives from 5 m pixel DTM of the Campania Region topographic map (CTR) at 1:5.000 scale.

Material and methods

Preliminary geomorphological analysis of the Punta Epitaffio area was conducted for the definition of morpho-structural setting and instability conditions of the cliff. In particular, a 5 m pixel digital elevation model, derived by Campania Region topographic map (CTR) at 1:5.000 scale (http://sit.provincia.napoli.it/cartografia_ctp98.html), was used to derive hillshade morphology, slope and aspect parameters. Structural field mapping of selected areas of the cliff, aided the recognition of morpho-structural elements detected on the basis of the DEM-derived attributes and orthophotograph interpretation.

The geomorphological study was integrated with the analysis of the ground deformation field of the study area derived by Synthetic Aperture Radar interferometry (InSAR) data from satellite ENVISAT for the period 2003-2010 [MATTM, 2015]. The InSAR data were processed according with the method of Persistent Scatterers Pair (PSP) [Costantini et al., 2008, 2009]. The PSP processing method identifies Persistent Scatterers (PS) from a series of full resolution SAR images, retrieves the corresponding terrain height and calculates average annual displacement velocity along Line of Sight (LOS) of the satellite sensor. In order to better constrain the ground deformation pattern at Punta Epitaffio cliff, which is actually exposed towards the East, we selected the ENVISAT descending orbit dataset which is characterized by a LOS with inclination of 25° with respect to the vertical and look from East to West.

The geostructural analysis was based on the method of automatic extraction of discontinuity orientation by TLS data, as proposed by Fanti et al. [2013] and partly modified in Matano et al. [2015]. To obtain a detailed 3D model of the coastal cliff, we used the TLS technique based on Time of Flight (TOF) method, which implies calculation of the two-way travel time of the laser pulse reflection from source/receiver to target, allowing for good accuracy and range of measurements [Abellàn et al., 2014]. Following the TLS acquisition, raw data were processed to obtain a point cloud, from which an interpolated 3-D surface (triangular mesh type) was created, where each element (facet) is characterized by a given orientation (dip/dip direction). Then a statistical grouping and classification of the facets was made on the basis of their spatial orientation, by using the "Open plot" software [Tavani et al., 2011].

Kinematic analysis for the definition of failure mechanisms was conducted using Dips 6.0 software [ROCSCIENCE, 2013]. Processing of the 3D model was addressed to the extraction of best-fit attitude (dip and dip direction) of discontinuity sets for each sub-planar patch of the rock face. Finally a cluster analysis of fitted planes [Hamman and Curran, 1998] was performed.

Geological, geomorphological and structural features of Punta Epitaffio area

The Punta Epitaffio cliff is located in the western sector of the coastal zone of the Pozzuoli Bay (Fig. 1). The Punta Epitaffio area is characterized by the outcrop of the "Epitaffio Yellow Tuff" formation (Fig. 2), also referred to as "Mofete Yellow Tuff", an ignimbritic deposit dated between 10.7 and 15.3 ka BP [Lirer et al., 2011]. In the north-eastern sector, the unit is formed by thin-bedded, welded pyroclastic deposits, including white vesicular pumice lenses within a yellowish sand-ashy matrix. Grain size variations within the stratigraphic succession locally produce differential erosion along the cliff profile. Bedding is characterised by sub-horizontal to slightly inclined strata with average direction N75-80°. In the southern sector a semi-coherent facies of the yellow tuff crops out (Fig. 2). The exposed succession is characterised at the top by ca. 10 m thick loose pyroclastic and colluvial deposits.

The small promontory of Punta Epitaffio separates two segments of the coastal cliff, exposed to the south and to the east, respectively (Figs. 2 and 3). The eastern sector of the cliff is about 50 m high and 400 m wide (Fig. 4a), while the southern sector is about 30 m high and 250 m wide (Fig. 4b). Both sectors are crossed halfway by a national road.

During the last decade both the cliff segments were affected by six main failures (Tab.

1; Figs. 2 and 3), which caused several interruptions of the traffic along the coast. Slope instability was mostly represented by tuff blocks and soil falls and slides from the upper part of the cliff, along with partial collapse of the roadway as a consequence of the progressive erosion and retreat of the lower part of the slope due to marine erosion at the base of the cliff. Several works were realized at Punta Epitaffio cliff, during the last years, mostly consisting in the reinforcement of the rockface by shotcrete, wire mesh and steel cable network applied to the tuff wall (Fig. 3).

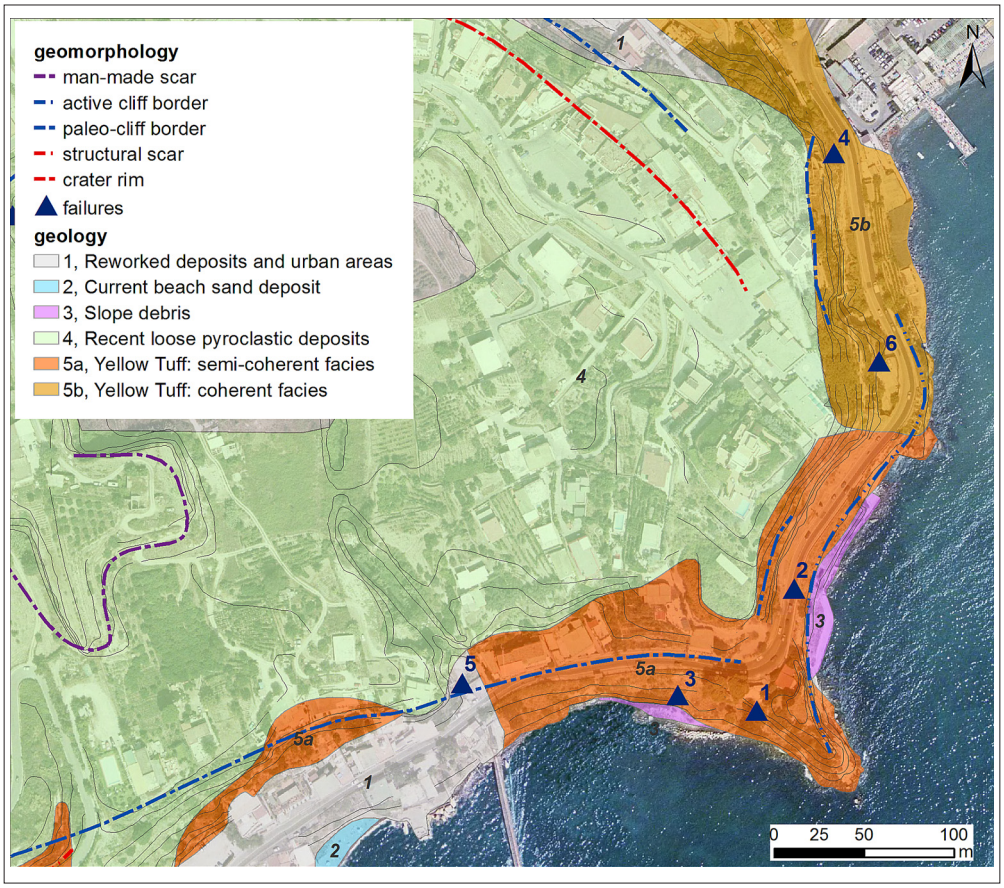

Figure 2 - Geological and geomorphological map of the Punta Epitaffio area.

The present work focuses on the central part of the eastern sector of Punta Epitaffio cliff (Figs. 3 and 4a) it represents the only segment of the coastal cliff that has not been subject to reinforcement works in the area (Fig. 3). In this sector, where the rockface is 30 m high and 60 m wide, stability problems remain partly unsolved, as also suggested by the information on the recent ground deformation trends derived by the analysis of the PSP dataset of ENVISAT satellite.

The ground deformation field obtained by available PSP data (descending orbit, 2003-2010

time period) suggests a general stability and/or slow subsidence of the Punta Epitaffio area with the notable exception of some targets located at the top of the eastern sector of the cliff, which are characterized by accelerated subsidence, in the order of -2.9 - 3.3 mm/year (average velocity) (Fig. 5).

Table 1 - Recent failure events at Punta Epitaffio.

Cliff sector	Date	Failure type	Triggering factor	Damages
1) Southern	2004	Rock fall	Unknown	Collapse of archaeological ruins (*Villa di Claudio*)
2) Eastern	2008-12	Rock fall	Coastal storm	National road closure for some weeks and cliff retreat
3) Eastern	2008-12-15	Rock fall	Heavy rain	National road closure for some weeks
4) Southern	2010-12-09	Rock fall	Wind and Heavy rain	Collapse of archaeological ruins (*Villa di Claudio*)
5) Southern	2013-07-03	Rock fall	Unknown	Collapse of archaeological ruins
6) Eastern	2014-01-22	Soil and rock fall	Heavy rain	National road closure for some days

In this area faults and structural discontinuity sets appear to exert a strong control on the morphological evolution of the tuff cliff and related failures (Tab. 1). The morphological analysis (Fig. 2) provided further evidence for diffused slope instability controlled by discontinuities in the rock mass, mostly associated with rock fall and rock slide mechanisms. In the studied cliff segments the failures are characterized by a frequency of about 0.5 event/yr with estimated involved volumes ranging between 10 and 100 m^3.

In order to recognize the discontinuity sets, a morpho-structural mapping was performed (Fig. 6). The morpho-structural analysis allowed for the definition of the average orientation values of the main observed structural sets, which are mostly steep and planar with variable spatial density:

a) Set K1 - average direction N110°-150°, sub-vertical and sub-orthogonal to the cliff;
b) Set K2 - average direction N60-80°, sub-vertical and sub-parallel to the cliff;
c) Set K3 - average direction N170°-190°, sub-vertical and sub-orthogonal to the cliff.

The structural origin of the discontinuity sets is genetically associated to both Neapolitan Yellow Tuff caldera volcano-tectonic deformation and NW-SE and NE-SW regional extensional structures (Acocella, 2010; Vitale and Isaia, 2014).

In this unstable sector (Fig. 4a) TLS surveys were executed (Fig. 7) and geostructural and kinematic analyses were performed in order to detect potential failure conditions and identify areas susceptible to different types of instability.

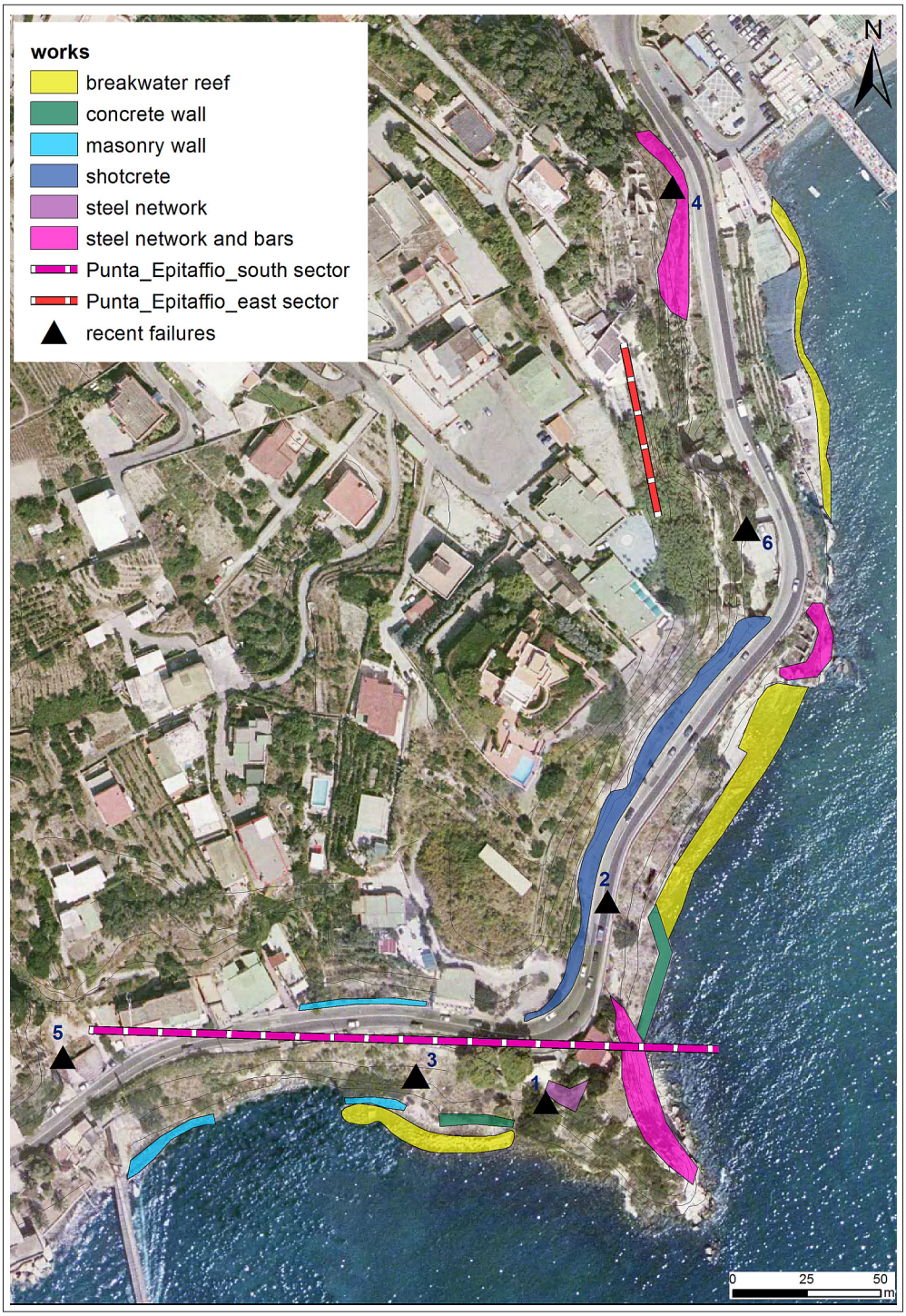

Figure 3 - Punta Epitaffio cliff sectors with location of the reinforcement works.

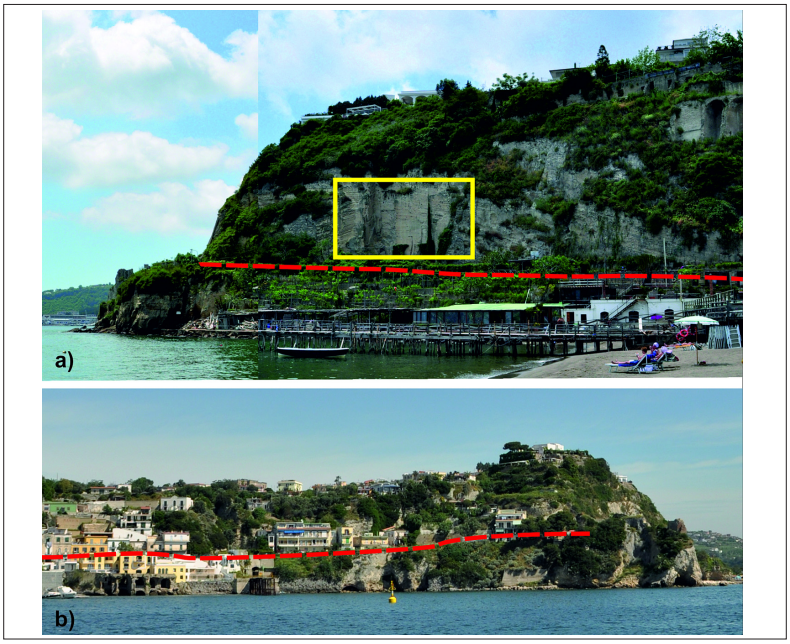

Figure 4 - Punta Epitaffio cliff photos: a) eastern side; b southern side. The yellow box shows the studied sector; the red dotted line shows the national road location.

Figure 5 - Ground deformation field during 2003-2010 time interval obtained by Persistent Scatterers Pair (PSP) radar interferometric data by the satellite Envisat - Descending orbit (data source: http://www.pcn.minambiente.it/viewer/index.php?project=ps_envisat_desc).

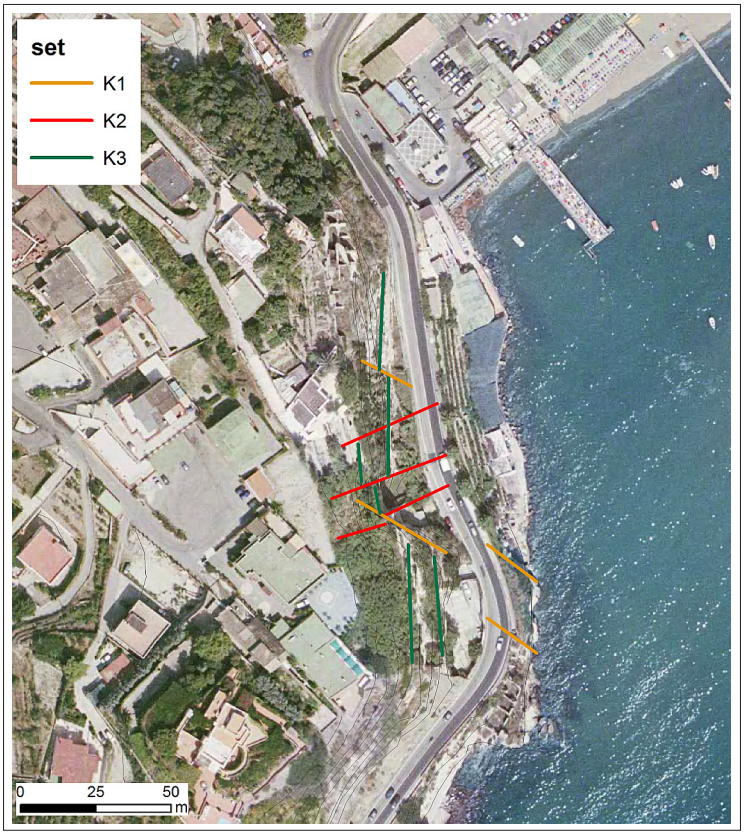

Figure 6 - Main fractures with morphological relevance along the studied sector of the cliff.

TLS data acquisition

TLS data were acquired with long-range laser scanner RIEGL VZ1000®. The instrument emits a narrow pulsed laser beam in SWIR (Shortwave Infrared) band (wavelength 1550 nm). The scanner is equipped with a 14 megapixel external digital camera NIKON D90®, which is mounted on the top of TLS with a holder system that ensures the contemporaneous acquisition of high resolution images and the 3D point cloud data.

The data acquisition included the following main steps: 1) Preliminary data acquisition and site inspection; 2) Topographic survey for georeferencing TLS data; 3) Laser scanning from fixed scan positions.

After considering the orientation and exposure of the rock cliff with respect to the coastline geometry and the possible location of scanning stations, seven different fixed stations were planned during the TLS survey in order to reduce occlusions and ensure direction of acquisition nearly normal to the rock surface. Consecutive scanning scenes were acquired with an overlap of at least 60%, to ensure a full coverage of the rock face.

A survey acquired with a Total Station LEICA TS12 3” R1000® supplied the topographic reference framework. The network in the study area consisted of 7 scan stations, 5 benchmarks, 4 artificial targets and 6 high-reflectivity natural targets. Considering that the

survey was conducted within a distance of observation up to ca. 500 m from the rock slope, the accuracy in the definition of the positions resulted in between 5 mm and 15 mm. All measurements were referred to UTM coordinate system (datum WGS84).

The scanning operations were carried out in a sunny day during late spring and the cliff surface was dry. The adopted laser scanning sensor has a field of view of 360° x 100° and a range capability up to 1.400 m for 90% reflectivity of the target for normal incidence condition of the beam on the target. As incidence increases, the range capability may be strongly reduced, depending on roughness of the target material. The yellow tuff of Punta Epitaffio cliff has an estimated average reflectivity of about 40 % for normal incidence conditions. Therefore by considering that our scan directions are near to the normal directions to acquired surfaces, in order to obtain an accuracy of 20 mm, the distance of the scanning stations from the cliff was limited in the range of 30 - 200 m. A total of nine scans of the entire cliff surface were acquired. The complete survey was carried out by three operators on 10 May 2013, during about 9 hours of data acquisition (from 8:00 a.m. to 4 p.m.).

During TLS operations the calibrated camera mounted on the laser scanner was used to acquire simultaneous photographic recording of the surveyed rock slope. The main outputs of the TLS data acquisition are RGB images and a raw 3-D point cloud of the cliff (Fig. 7a) with a point density of 2 cm^{-2}. The digital photographs acquired during the TLS survey were processed in order to extract vertical orthophotos of the rock face [Neteler et al., 2005]. RGB images of the surveyed area were then used for the texturing of the point cloud during the post-processing phase (Fig. 7b).

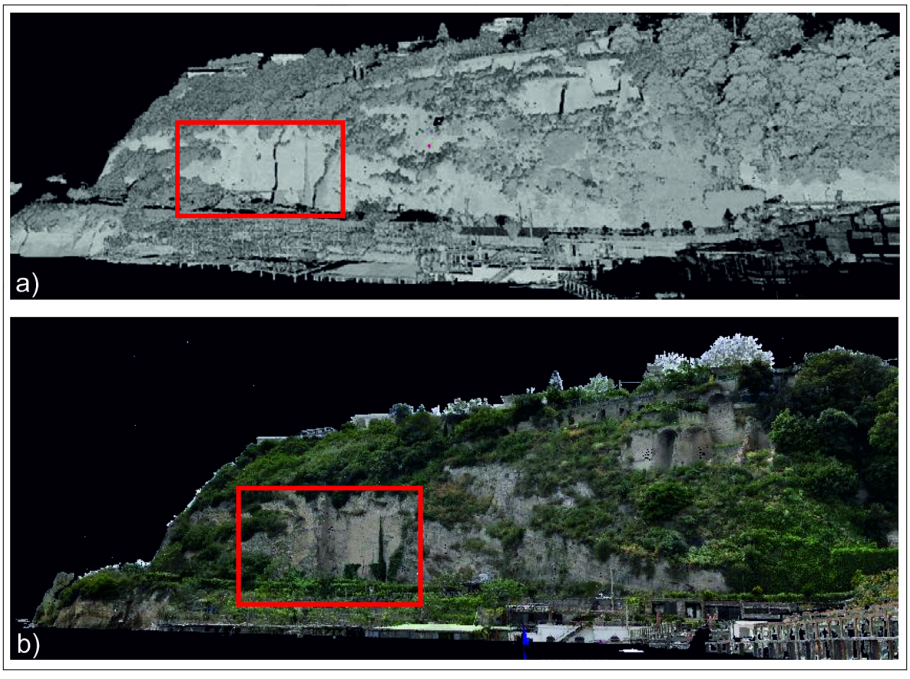

Figure 7 - a) Raw point cloud with intensity output values obtained by RiSCAN PRO software (RIEGL, 2011); b) Raw point cloud matched with colour RGB images. The red box shows the studied sector of the cliff.

TLS data processing

TLS data processing consisted in four main steps: 1) processing of the point cloud data (filtering, registration and decimation) and matching with RGB images; 2) implementation of a 3D model (triangle mesh) of the rock face; 3) GIS processing to obtain orientation data required for geostructural analysis; 4) development of a 2.5D Triangular Irregular Network (TIN) in a vertical orthometric projection; 5) interpolation of a DEM from the TIN.

In order to acquire a point cloud within a specific coordinate system, and available for further analysis [Abellàn et al., 2014], TLS raw data were processed using the RiSCAN PRO® software [RIEGL, 2011]. Filtering of the dataset consisted in the removal of non-ground points (vegetation, steel nets, etc.) through an automatic noise reduction filter and then manual editing. This operation is necessary in order to obtain the rock surface morphology and to allow a correct extraction of geostructural information from the 3D model derived by TLS data.

Registration of the acquired point cloud included the union of the contiguous nine scans in a unique dataset and its georeferencing [Abellàn et al., 2014]. The alignment of individual scans was obtained by using ICP algorithm of RiSCAN PRO® software (RIEGL, 2011), with consequent reduction of occlusion effects. Georeferencing of the point cloud in the UTM projection system (datum WGS84) was ensured by the recognition, in the point cloud, of the calibrated targets previously geo-referenced by DGPS or total station positioning.

The point cloud sampling density was subsequently reduced (decimation) from 1 point/2 cm^2 to 1 point/5 cm^2 over the entire area. This operation was aimed at: a) optimizing the sampling density with respect to the required spatial resolution, which is linked to the minimum expected size of interesting features (10 cm); b) decreasing the overlap of points derived from different scans and c) reducing the weight of computing operations. Moreover, the point cloud was coloured by matching the dataset with the RGB images captured by the calibrated camera during the scans (Fig. 7b).

Further processing consisted in the implementation of a detailed 3D digital model (triangle mesh) of the rock face (Fig. 8a), without interpolated surfaces, by processing with MESHLAB® software (VCG, 2013) the clean point cloud, filtered from vegetation. In the 3D model (triangle mesh) each triangular facet is characterized by its spatial orientation (dip and dip direction) and elevation (ellipsoidal height) data. These data are relevant for characterizing the geo-structural conditions of the rocky cliff surface.

In order to assign this spatial information to each polygon of the 3D model and derive orientations for each portion of the rock front, the 3D mesh was imported in ArcGIS as polygon file, where each feature of the triangular polygon file corresponds to a facet of the mesh. Then a GIS processing (i.e. spatial analysis tool; ESRI, 2012) was carried out. Orientation data were georeferenced with respect to the geographic north and the horizontal plane. In this way, values for steepness (inclination or dip-angle) and aspect (azimuth or dip-direction) were assigned to each polygon. The computed dip directions and dip angle of 3D facets were then used for queries.

The use of ArcMap® software (ESRI, 2012) allowed for further processing of the 3D point cloud data to obtain a 2.5 D TIN (Fig. 8b) in a vertical orthometric projection. In order to generate the desired vertical TIN, the 3D point cloud data were preliminarily georeferenced in a local coordinate system where a projection plane, representing the base level of the TIN, was defined parallel to the cliff. The TIN was used to derive topographic features and vertically projected raster images.

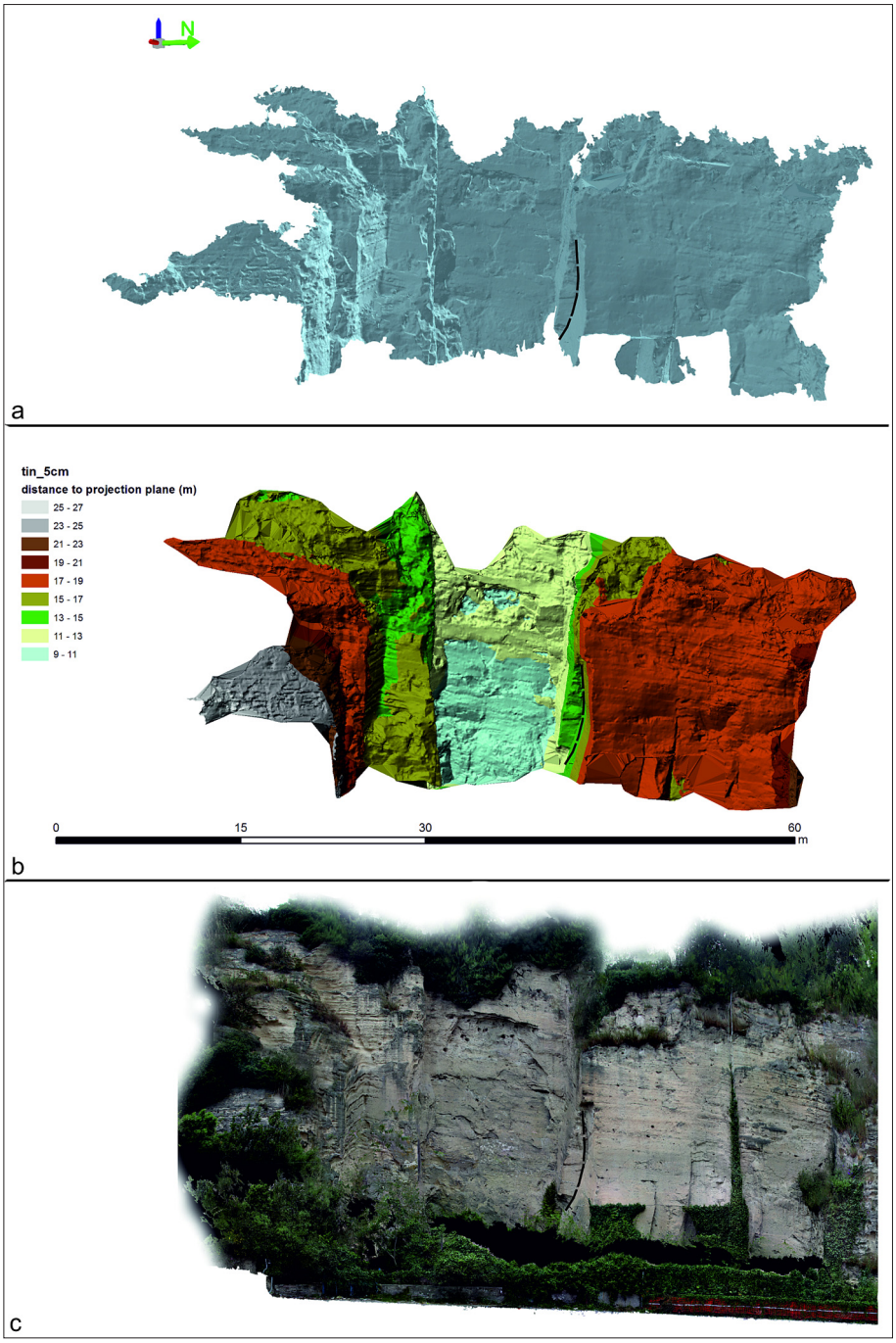

Figure 8 - Punta Epitaffio tuffaceous cliff models: a) 3D model (triangular mesh); b) TIN terrain model; c) orthophoto. See the dotted black line for comparison. The images were elaborated with ArcMap software (ESRI, 2012).

Based on the TIN, a raster DEM was elaborated where contiguous pixels have a fixed size of 5 cm and all pixels preserve the spatial information in a positioning matrix, represented by a Cartesian reference system that includes elevation data. Photographs acquired with the high-resolution calibrated camera were used to derive an RGB composite image of the frontal view of the cliff (Fig. 8c). This image was obtained by orthorectification of the photomosaic, using the DEM as a reference [Neteler et al., 2005].

TLS data analysis

The analysis of TLS data acquired at Punta Epitaffio provided a means for a better definition of the discontinuity sets defined with the morphostructural analysis and a good constraint for failure kinematics recognized during the field mapping.

Data analysis consisted in the following main steps: 1) statistical analysis of spatial orientation of the facets of the mesh; 2) definition of the major discontinuity sets by data classification; 3) geo-structural classification of 3D model facets in GIS environment.

The identification and mapping of the major discontinuity sets was carried out through a statistical analysis conducted on all the polygons (ca. 1.6 millions) forming the triangle mesh of the 3D model, using the "Open plot" software [Tavani et al., 2011].

Statistical analysis has allowed for identification of three main clusters of facets orientation in the 3D mesh (Fig. 9), with the following average dip directions: a) 160-170° or 340-350°, b) 60-70° or 240-250°, and c) 180-190° or 0-10°.

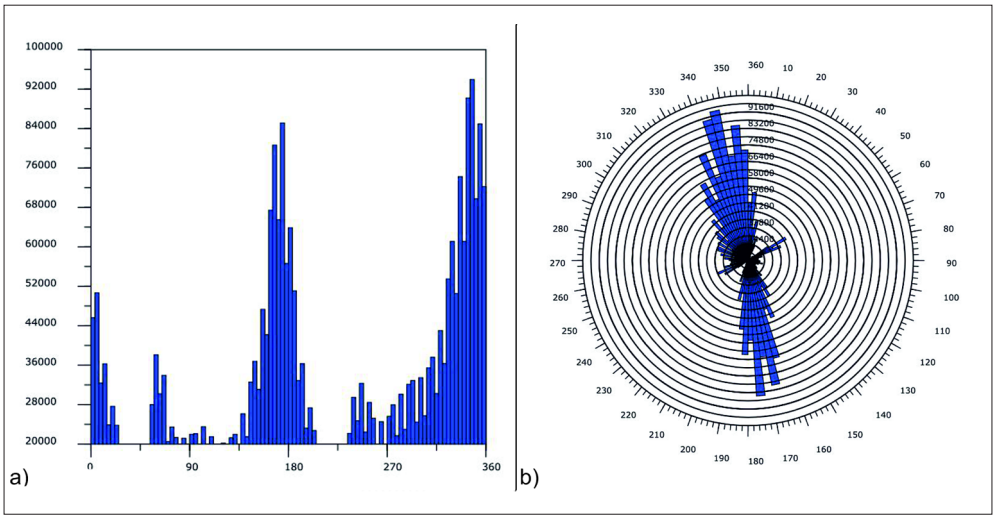

Figure 9 - Results of statistical analysis of dip direction values distribution performed with "Open Plot" software [Tavani et al., 2010]: a) histogram; b) rose diagram.

We used the same names for structural sets derived by photo-interpretation and TLS data because the integrated analytical approach adopted in this study highlights a good correlation between the two dataset (Figg. 6, 9 and 10). Rather, the orientation clusters permitted a better definition of the three already recognized main discontinuity sets (Fig. 10):

− K1, characterized by dip direction 140°/170° and 320°/350° (sub-parallel to the cliff), dip >75°, sub-vertical;
− K2, characterized by dip direction 235°/280° and 65°/95° (sub-orthogonal to the cliff), dip >70°, sub-vertical;
− K3, characterized by dip direction 185°/210° and 0°/30° (sub-orthogonal to the cliff), dip >70°, sub-vertical.

The defined discontinuity sets were selected and classified on the 3D model mesh with the use of ArcGIS® software (ArcScene) to obtain a 3D geo-structural model. A series of spatial queries allowed for the overlapping of the discontinuity sets and the morphological features of the 3D model in the different sectors of the cliff. In Figures 11, 12 and 13 various perspectives are illustrated with different vertical and horizontal angles of view in order to show an overall view of the 3D distribution of the recognized joint sets (Figs. 11 and 12) and bedding (Fig. 13) along the cliff surface.

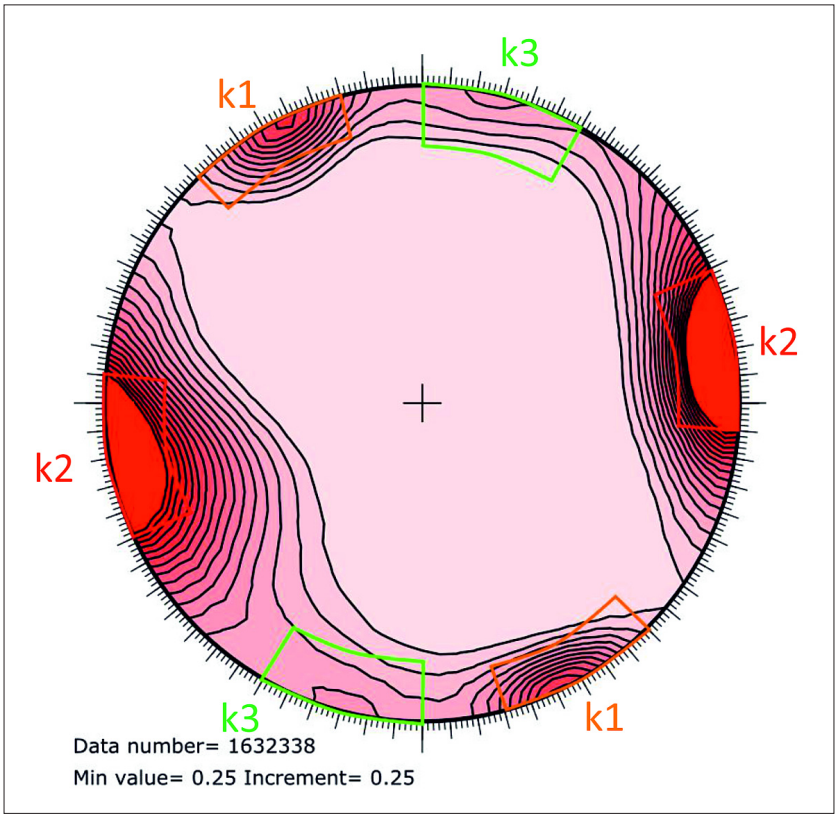

Figure 10 - Density diagram (K1 - orange box, K2 - red box, K3 - green box) by OpenPlot software [Tavani et al., 2011].

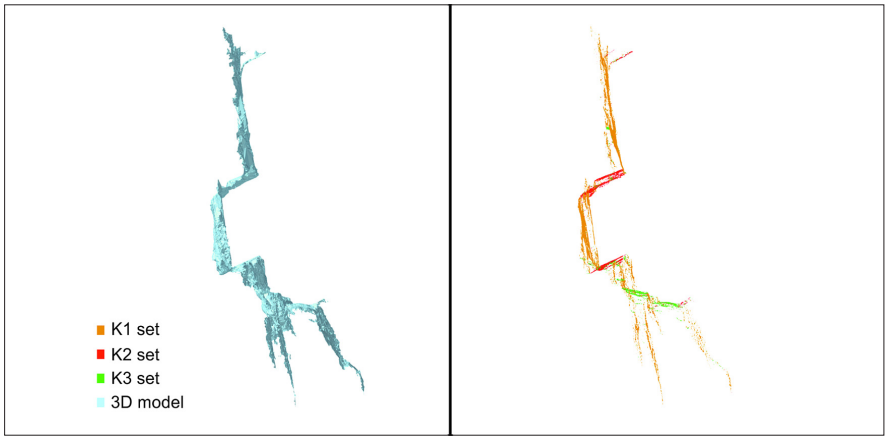

Figure 11 - 2D view of the geostructural model with subvertical sets K1-K2-K3. The images were elaborated with ArcMap software (ESRI, 2012).

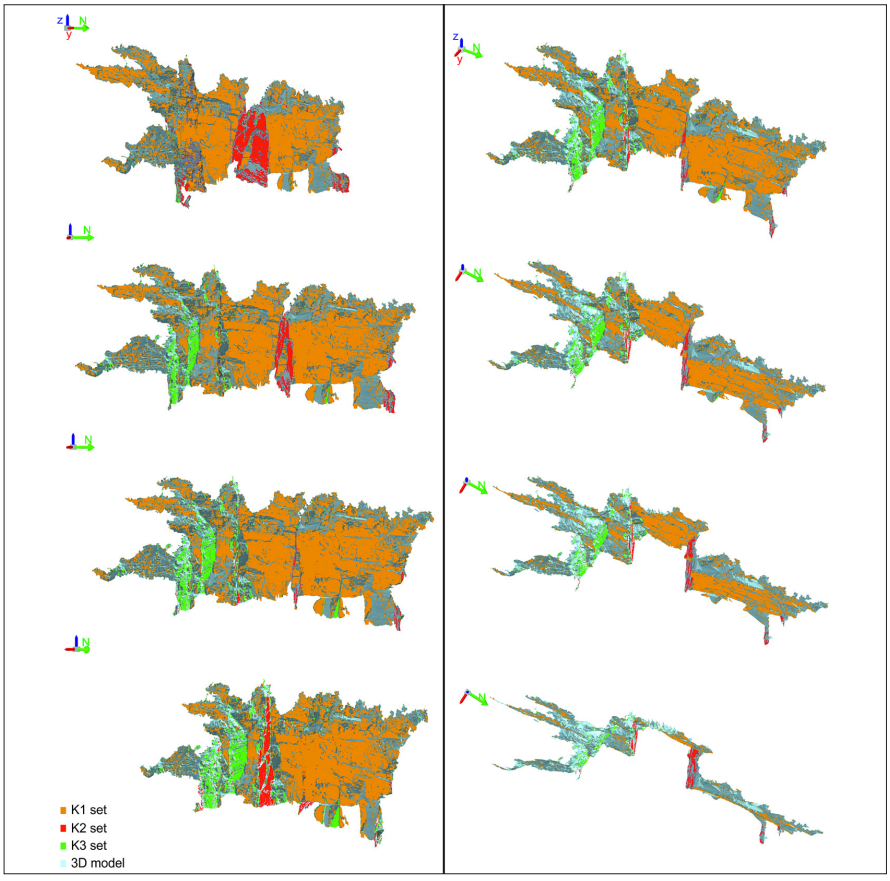

Figure 12 - Perspectives with different vertical and horizontal angles of the 3D geostructural model with subvertical sets K1-K2-K3. The images were elaborated with ArcMap software (ESRI, 2012).

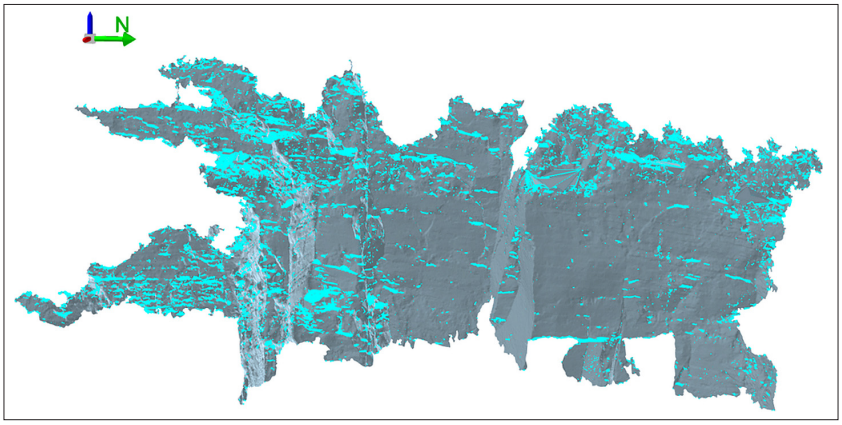

Figure 13 - Frontal perspective of the 3D geostructural model with little morphological evidence of sub-horizontal bedding and joints. The image was elaborated with ArcMap software (ESRI, 2012).

Failure kinematic analysis

The results obtained from the statistical analysis of the 3D geostructural model suggest that this dataset, after appropriate statistical filtering, can be successfully used for failure kinematic analysis. However, caution must be used in order to avoid a statistical bias linked to the extension of surfaces controlled by structural discontinuities. This drawback can be resolved by considering the real number of structural discontinuities in failure analyses and the 3D model was processed in order to derive the best-fit planes for each sub-planar patch of the rock face. According with this procedure, 360 sub-planar patches were detected and fitted by planes from which orientation data were extracted. Cluster analysis [Hamman and Curran, 1998] of fitted planes clearly shows the already recognized three sets of discontinuities (K1, K2, K3), as well as additional sets characterized by relatively minor morphological expression (Fig. 14). The full list of recognized sets can be described as follows:

− K1, characterized by ranges of dip directions of 145-180° and 320-350° and dip angle varying between 75° and 90°;

− K1a, characterized by dip directions varying between 145-185° and dip angle varying between 55° and 75°;

− K1b, characterized by dip directions varying between 320-350° and dip angle varying between 55° and 70°;

− K2, characterized by dip directions varying between 60° and 100° and dip angle varying between 55° and 90°;

− K2a, characterized by dip directions varying between 65-95 and 235-270° and dip angle varying between 30° and 60°;

− K3, characterized by dip directions varying between 355-30° and 190-220° and dip angle varying between 70° and 90°;

− K3a, characterized by dip directions varying between 190-220° and dip angle varying between 30° and 70°;

− K4, characterized by dip direction varying between 100-120° and 270-310° with dip angles > 65°;

− K4a, characterized by dip directions varying between 95-130° and dip angles varying between 45° and 75°;
− K5, characterized essentially by dip directions varying between 35-65° and 225-245° and dip angles > 65°.

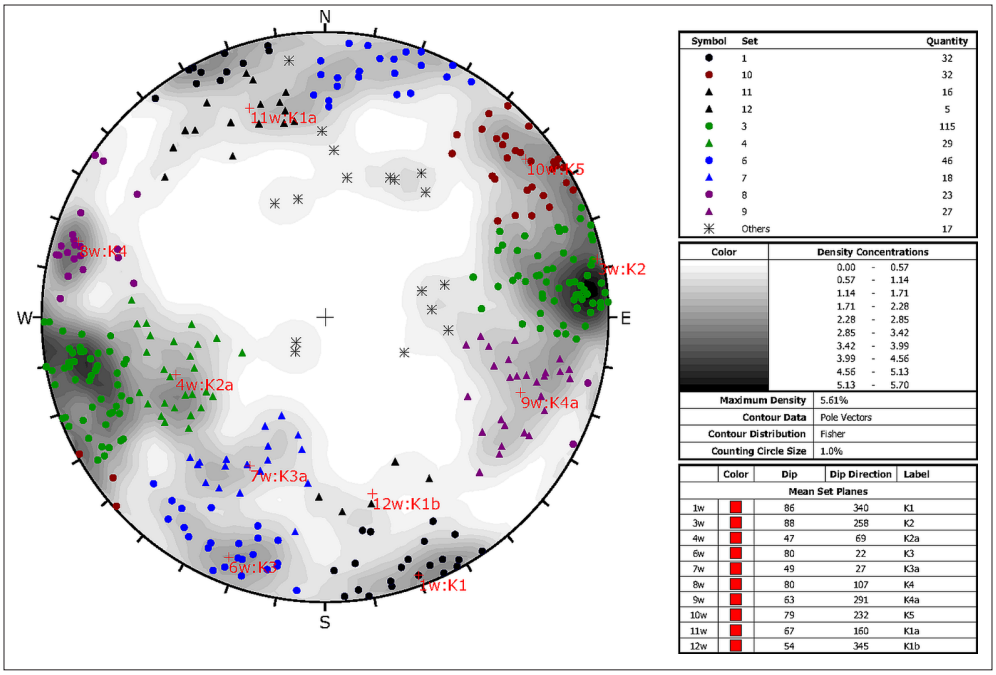

Figure 14 - Synthetic stereonet for all discontinuity sets derived by the global cluster analysis, by Dips software [ROCSCIENCE, 2013].

These data display a good correlation with contour-plots of 3D facets (Fig. 10) with particular reference to the prominent clusters associated with the three main vertical sets (K1, K2 and K3). Among the additional set of identified clusters, some (i.e. K1a, K1b, K2a, K3a,) are geometrically related to the main vertical sets (even though they display lower dip angle), while others (i.e. K4, K4a and K5) correspond to new sets. The detected sets are likely related to fractures characterized by limited morphological extension, and they are therefore overlooked in the 3D facets analysis by the statistical relevance of facets pertaining to larger planar surfaces.
Failure kinematic analysis was based on data derived from the best-fit plane detection, considering the main failure criteria (Fig. 15), such as planar sliding [Goodman, 1980; Hudson and Harrison, 1997], wedge sliding [Markland, 1972], flexural toppling [Goodman, 1980], and direct toppling [Hudson and Harrison, 1997].
Kinematic analysis showed that planar sliding is possible by slip along fractures pertaining primarily to the K4a set, whose data fall by 93% of the cases within the area characterized by the most critical stability conditions, and subordinately pertain to the K2 and K4 sets (Fig. 15a).
Rock wedge sliding analysis shows full failure susceptibility, as more than 30% of

intersections fall within the critical areas both considering average plane sets or single planes. The most important wedge failures may be induced by the following series of structural intersections: a) K1a vs K4; b) K1a vs K3; c) K1a vs K2a; d) K1 vs K4; e) K1 vs K2a; f) K1 vs K3a; g) K3 vs K2a. They represent more than 50% of the possible intersections falling within the critical sector (Fig. 15b).

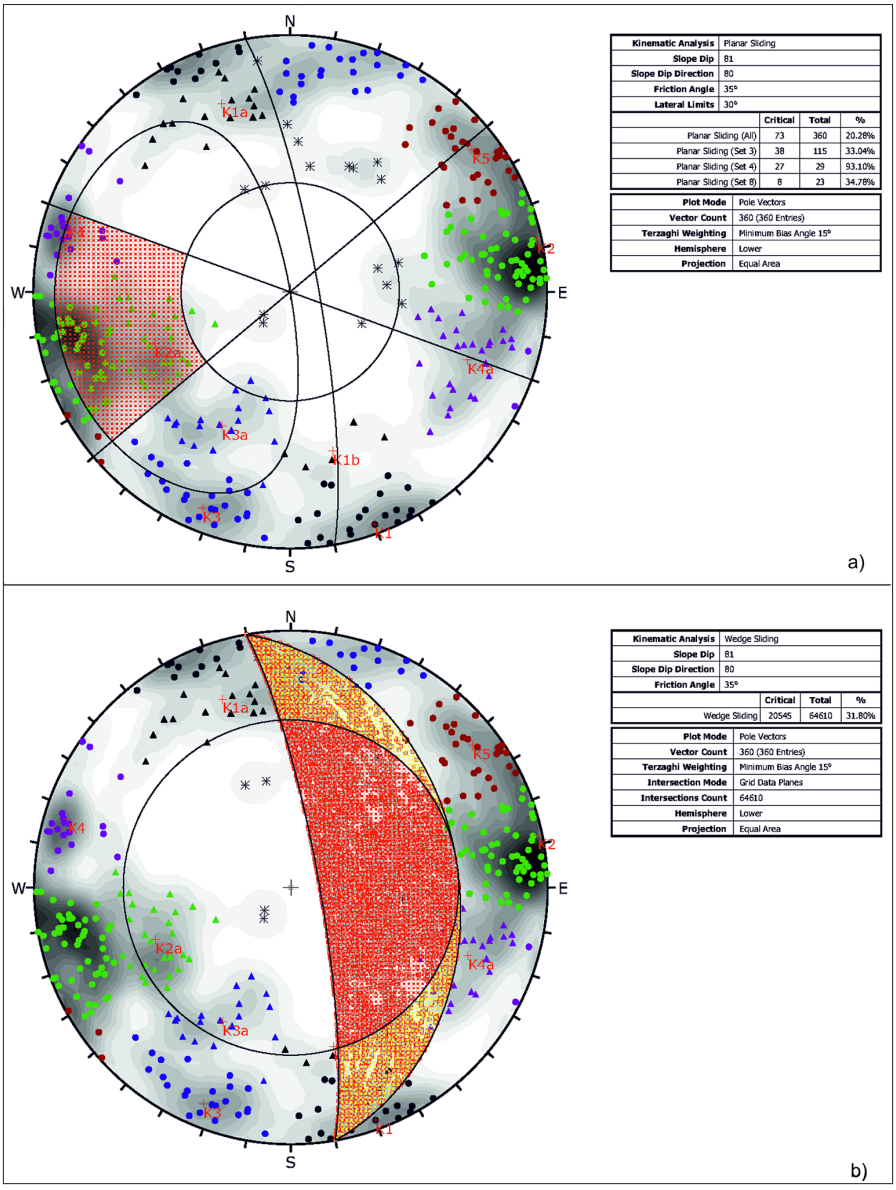

Figure 15 (Continued on next page) - Kinematic analysis for different failures criteria: a) planar sliding, b) wedge sliding, c) flexural toppling, d) direct toppling, by Dips software [ROCSCIENCE, 2013]. For symbols see Figure 14.

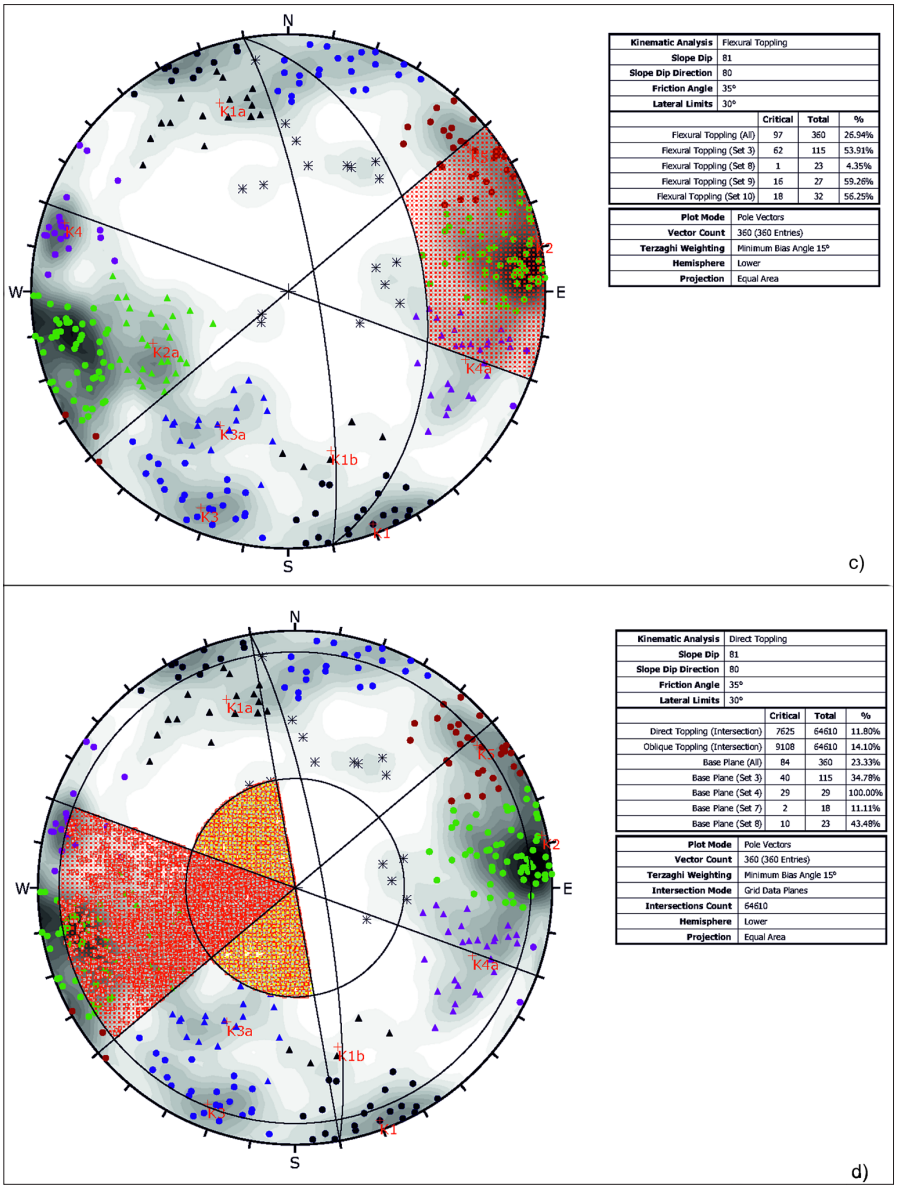

Kinematic Analysis	Flexural Toppling
Slope Dip	81
Slope Dip Direction	80
Friction Angle	35°
Lateral Limits	30°

	Critical	Total	%
Flexural Toppling (All)	97	360	26.94%
Flexural Toppling (Set 3)	62	115	53.91%
Flexural Toppling (Set 8)	1	23	4.35%
Flexural Toppling (Set 9)	16	27	59.26%
Flexural Toppling (Set 10)	18	32	56.25%

Plot Mode	Pole Vectors
Vector Count	360 (360 Entries)
Terzaghi Weighting	Minimum Bias Angle 15°
Hemisphere	Lower
Projection	Equal Area

Kinematic Analysis	Direct Toppling
Slope Dip	81
Slope Dip Direction	80
Friction Angle	35°
Lateral Limits	30°

	Critical	Total	%
Direct Toppling (Intersection)	7625	64610	11.80%
Oblique Toppling (Intersection)	9108	64610	14.10%
Base Plane (All)	84	360	23.33%
Base Plane (Set 3)	40	115	34.78%
Base Plane (Set 4)	29	29	100.00%
Base Plane (Set 7)	2	18	11.11%
Base Plane (Set 8)	10	23	43.48%

Plot Mode	Pole Vectors
Vector Count	360 (360 Entries)
Terzaghi Weighting	Minimum Bias Angle 15°
Intersection Mode	Grid Data Planes
Intersections Count	64610
Hemisphere	Lower
Projection	Equal Area

Figure 15 (Continued from preceding page) - Kinematic analysis for different failures criteria: a) planar sliding, b) wedge sliding, c) flexural toppling, d) direct toppling, by Dips software [ROCSCIENCE, 2013]. For symbols see Figure 14.

Flexural toppling, which is a relatively common failure mode in soft, poorly fractured rocks such as tuffs, may also occur at Punta Epitaffio cliff due to high angle joints pertaining mainly to K2a (100% critical), K4 (44% critical) and K3 sets (35% critical) (Fig. 15c).
The occurrence of sub-horizontal discontinuities, and intersecting vertical sets, can induce direct toppling. In this case, block slipping may occur along intersection between following

sets: K1 vs K4a (84% critical) ; K1 vs K5 (51% critical); K3 vs K4a (40% critical). Fractures systems potentially responsible for block releasing, are also associated with K2 (35% critical), K2a (100% critical) and K4 (44% critical) sets as well as to bedding surfaces, when disjunctive joints occur (Fig. 15d).
The data show that sets K2 and K4, and associated sub-sets K4a and K2a, contribute to all the tested failure modes, whereas set K1 contributes to wedge failures and direct toppling, where it intersects other systems (mainly K2, K3, and K4). Fractures belonging to the other sets are of relatively minor importance.

Discussion and conclusive remarks

Processing and interpretation of the TLS dataset was completed in eight working days, using a 64 bit workstation, with an Intel Xeon CPU 3.07 GHz and 6 GB RAM. A first output of TLS processed data consisted in a high-resolution 3D digital model (triangular mesh) of the Punta Epitaffio tuff cliff. Numerical integration of slope angles with the spatial attitude of the triangular facets of the mesh was used to obtain a 3D geo-structural model, where each facet is associated with a discontinuity set on the basis of its spatial attitude (dip direction and angle of dip) (Figs. 11, 12, 13).
The 3D model shows the cliff morphology with the preferential spatial orientation of planar-like patches of the rock surface that can be correlated with discontinuities sets within the rock (e.g. fractures, faults planes, bedding or morphological surfaces, etc.) according to classes of orientation (dip and dip direction).
The analysis of structural discontinuities on the 3D model showed a significant correlation between rock discontinuity sets detected by the TLS survey and families of fractures observed on the cliff with the morphostructural analysis. This allowed the use of the same names for structural sets derived by photo-interpretation and TLS data processing.
In order to detect potential failure conditions and identify areas susceptible to different types of instability, a kinematic analysis was performed and unstable tuff blocks and wedges, predisposing the cliff to rock failures, were recognized. In particular the failure susceptibility was tested for both single fracture data and main set data showing the high relevance of the sets K1, K2 and K4 for their contribution to slope instability.
The main results obtained in this study can be summarized as follows:
1) Geomechanical analysis of the tuff coastal cliff was fully conducted in remote, (i.e. under safety conditions for operators), whereas other approaches invariably require a direct access to the investigated rock front;
2) TLS accuracy, precision and resolution are adequate and consistent for the scope of geomechanical analysis;
3) An assessment of rockfall susceptibility was obtained for the Punta Epitaffio tuff cliff on the basis of a Terrestrial Laser Scanning survey.
The kinematic analysis data show that sets K2 and K4, and associated sub-sets K4a and K2a, contribute to all the tested failure modes, such as planar sliding, wedge sliding, flexural and direct toppling, whereas set K1 contributes to wedge failures and direct toppling, where it intersects other systems (mainly K2, K3, and K4).
The TLS acquired dataset also represent an archive database and reference for constraining the study of the evolution of the rock mass morphology in the perspective of multi-temporal integrated surveys including future TLS campaigns and the installation of both punctual

(strain gauge, inclinometer, crackmeter, load cell, etc.) and areal (fiber optic networks, etc.) monitoring sensors.

Acknowledgements

This work was supported by the Programma Operativo Nazionale (PON) funded by the Italian Ministries of University and Research and Economic Development - Project PON-MONICA (grant PON01_01525). Satellite ENVISAT data were provided by *Extraordinary Plan of Environmental Remote Sensing - Geoportale Nazionale*, Ministero per la Tutela dell'Ambiente, del Territorio e del Mare. We wish to thank editors and the two anonymous reviewers who helped us improve the early version of the manuscript.

References

Abellán A., Oppikofer T., Jaboyedoff M., Rosser N. J., Lim M., Lato M.J. (2014) - *Terrestrial laser scanning of rock slope instabilities*. Earth Surface Processes and Landforms, 39: 80-97. doi: http://dx.doi.org/10.1002/esp.3493.

Acocella V. (2010) - *Evaluating fracture patterns within a resurgent caldera: Campi Flegrei, Italy*. Bulletin of Volcanology, 72: 623-638. doi: http://dx.doi.org/10.1007/s00445-010-0347-x.

Barbarella M., Fiani M. (2013) - *Monitoring of large landslides by Terrestrial Laser Scanning techniques: field data collection and processing*. European Journal of Remote Sensing, 46: 126-151. doi: http://dx.doi.org/10.5721/EuJRS20134608.

Beneduce P., D'Elia G., Guida M. (1988) - *Morfodinamica dei versanti dell'area flegrea (Campania): erosione in massa ed erosione lineare*. Memorie della Società Geologica Italiana, 41: 949-961.

Bitelli G., Dubbini M., Zanutta A. (2004) - *Terrestrial Laser Scanning And Digital Photogrammetry Techniques To Monitor Landslide Bodies*. Proceedings of the XXth ISPRS congress, Istanbul, Turkey. Commission V, WG V/2.

Costantini M., Falco S., Malvarosa F., Minati F. (2008) - *A new method for identification and analysis of persistent scatterers in series of SAR images*. Proceedings of the International Geoscience and Remote Sensing Symposium, Boston MA, USA, 7-11 July 2008, pp. 449-452. doi: http://dx.doi.org/10.1109/igarss.2008.4779025.

Costantini M., Falco S., Malvarosa F., Minati F., Trillo F. (2009) - *Method of Persistent Scatterer Pairs (PSP) and high resolution SAR interferometry*. Proceedings of the International Geoscience and Remote Sensing Symposium, 3: 904-907. doi: http://dx.doi.org/10.1109/igarss.2009.5417918.

De Natale G., Troise C., Pingue F., Mastrolorenzo G., Pappalardo L., Battaglia M., Boschi E. (2006) - *The Campi Flegrei caldera: unrest mechanisms and hazards*. Geological Society, London, 269: 25-45. doi: 10.1144/GSL.SP.2006.269.01.03. doi: http://dx.doi.org/10.1144/GSL.SP.2006.269.01.03.

Del Gaudio C., Aquino I., Ricciardi G.P., Ricco C., Scandone R. (2010) - *Unrest episodes at Campi Flegrei: A reconstruction of vertical ground movements during 1905-2009*. Journal of Volcanology and Geothermal Research, 195: 48-56. doi: http://dx.doi.org/10.1016/j.jvolgeores.2010.05.014.

Esposito G., Iuliano S., Marino E., Matano F., Pignalosa A., Sacchi M., Sarnacchiaro G. (2013) - *Rilievi con tecnica laser-scanner nell'area flegrea per il monitoraggio dei*

costoni tufacei e dei fondali adiacenti. In: "Riassunti del Congresso AIQUA 2013 - L'ambiente Marino Costiero del Mediterraneo oggi e nel recente passato geologico. Conoscere per comprendere. Napoli 19-21 giugno 2013". Miscellanea INGV, 19: 129.

ESRI (2012) - *Arc GIS, ArcMap software, version 10.1*. Environmental Systems Resource Institute (ESRI), Redlands, California, USA. Available online at: www.esri.com

Evangelista A., Scotto Di Santolo A., Zimbardo M., Ercoli L., Nocilla N. (2010) - *Influence of the behaviour of soft rocks on cliff evolution. Rock Mechanics in Civil and Environmental Engineering*. Proceedings of the European Rock Mechanics Symposium, EUROCK 2010, 643-646; Lausanne (Switzerland), 15-18 June 2010.

Fanti R., Gigli G., Lombardi L., Tapete D., Canuti P. (2013) - *Terrestrial laser scanning for rockfall stability analysis in the cultural heritage site of Pitigliano (Italy)*. Landslides, 10: 409-420. doi: http://dx.doi.org/10.1007/s10346-012-0329-5.

Goodman R.E. (1980) - *Introduction to Rock Mechanics*. John Wiley (Ed.), Toronto, Chapter 8: 254-287.

Hammah R.E., Curran, J.H. (1998) - *Fuzzy Cluster Algorithm for the Automatic Identification of Joint Sets.* International Journal of Rock Mechanics & Mining Sciences,35 (7): 889-905. doi: http://dx.doi.org/10.1016/S0148-9062(98)00011-4.

Hudson J.A., Harrison J.P. (1997) - *Engineering Rock Mechanics - An Introduction to the Principles*. Pergamon Press.

Hunter G., Pinkerton H., Airey R., Calvari, S. (2003) - *The application of a long-range laser scanner for monitoring volcanic activity on Mount Etna*. Journal of Volcanology and Geothermal Research, 123: 203-210. doi: http://dx.doi.org/10.1016/S0377-0273(03)00036-2.

Lim M., Rosser N.J., Allison R.J., Petley D.N. (2010) - *Erosional processes in the hard rock coastal cliffs at Staithes North Yorkshire*. Geomorphology, 114: 12-21. doi: 1 http://dx.doi.org/10.1016/j.geomorph.2009.02.011.

Lirer L. (2011) - *I Campi Flegrei. Storia di un campo vulcanico*. Quaderni dell'Accademia Pontaniana, 57: 1-178, Napoli.

Lirer L., Petrosino P., Alberico I. (2001) - *Hazard assessment at volcanic fields: the Campi Flegrei case history*. Journal of Volcanology and Geothermal Research, 112: 53-73. doi: http://dx.doi.org/10.1016/S0377-0273(01)00234-7.

Markland J.T. (1972) - *A useful technique for estimating the stability of rock slopes when the rigid wedge slide type of failure is expected*. Imperial College Rock Mechanics Research Reprints, 19.

Matano F., Somma R., Marino E., Pignalosa A., Esposito G., Caputo T., Sacchi M., De Natale G. (2014) - *Laser Scanning Applications for Monitoring Tuffaceous Coastal Cliff in the Pozzuoli Bay, Punta Epitaffio Site, Italy: preliminary results*. In: Humair F., Matasci B., Jaboyedoff M., Abellan A., Carrea D., Derron M.-H., Guerin A., Michoud C., Nicolet P., Nguyen L., Penna I., Voumard J., Wyser M. (Eds.), Vertical Geology, from remote sensing to 3D geological modelling. Proceedings of the first Vertical Geology Conference 2014, 5-7 February 2014, University of Lausanne, Switzerland, pp. 207-212.

Matano F., Iuliano S., Somma R., Marino E., Del Vecchio U., Esposito G., Molisso F., Scepi G., Grimaldi G.M., Pignalosa A., Caputo T., Troise C., De Natale G., Sacchi M. (2015) - *Geostructure of Coroglio tuff cliff, Naples (Italy) derived from terrestrial laser scanner data*. Journal of Maps, published online 07 April 2015. doi: http://dx.doi.

org/10.1080/17445647.2015.1028237.

MATTM (2015) - *Extraordinary Plain of Environmental Remote Sensing (EPRS-E).* The National Geoportal (NG) of the Italian Ministry of Environment and of Protection of Territory and Sea . Available online at: http://www.pcn.minambiente.it/GN/progetto_pst.php?lan=en.

Neteler M., Grasso D., Michelazzi I., Miori L., Merler S., Furlanello C. (2005) - *An integrated toolbox for image registration, fusion and classification*. International Journal of Geoinformatics, 1 (1): 51-61.

Olsen M.J., Johnstone E., Driscoll N., Ashford S.A., Kuester F. (2009) - *Terrestrial laser scanning of extended cliff sections in dynamic environments: parameter analysis*. Journal of Surveying Engineering, 135 (4): 161-169. doi: 10.1061/(ASCE)0733-9453.

Orsi G., De Vita S., di Vito M. (1996) - *The restless, resurgent Campi Flegrei nested caldera (Italy): constraints on its evolution and configuration*. Journal of Volcanology and Geothermal Research, 74 (3-4): 179-214. doi: http://dx.doi.org/10.1016/S0377-0273(96)00063-7.

RIEGL (2011) - *RiSCAN PRO software, version 1.7*. RIEGL Laser Measurement Systems GmbH, www.riegl.com; Horn, Austria.

ROCSCIENCE (2013) - *Dips software, version 6.0, Graphical & Statistical Analysis of Orientation Data*. ROCSCIENCE Software tools for rock and soil. Available online at: https://www.rocscience.com/products/1/Dips; Toronto, Canada.

Sacchi M., Pepe F., Corradino M., Insinga D., Molisso F., Lubritto C. (2014) - *The Neapolitan Yellow Tuff caldera offshore the Campi Flegrei: Stratal architecture and kinematic reconstruction during the last 15 ky*. Marine Geology, 354: 15-33. doi: http://dx.doi.org/10.1016/j.margeo.2014.04.012.

Somma R., Matano F., Marino E., Caputo T., Esposito G., Caccavale M., Carlino S., Iuliano S., Mazzola S., Molisso F., Sacchi M., Troise C., De Natale G. (2014) - *Application Of Laser Scanning For Monitoring Coastal Cliff Instability In The Pozzuoli Bay, Coroglio Site, Posillipo Hill, Naples*. In: Lollino G., Manconi A., Guzzetti F., Culshaw M., Bobrowsky P., Luino F.(Eds.), Engineering Geology for Society and Territory,5 (133). doi: http://dx.doi.org/10.1007/978-3-319-09048-1_133.

Tavani S., Arbues P., Snidero M., Carrera N., Muñoz J.A. (2011) - *Open Plot Project: an open-source toolkit for 3-D structural data analysis*. Solid Earth, 2: 53-63. doi: http://dx.doi.org/10.5194/se-2-53-2011.

Young A.P., Guza R.T., O'Reilly W.C., Flick R.E., Gutierrez R. (2011) - *Short-term retreat statistics of a slowly eroding coastal cliff*. Natural Hazards and Earth System Sciences, 11: 205-217. doi: http://dx.doi.org/10.5194/nhess-11-205-2011.

VCG (2013) - *MeshLab software, version 1.3*. Visual Computing Lab, Istituto di Scienza e Tecnologie dell'Informazione (ISTI), Consiglio Nazionale delle Ricerche (CNR), Available online at: http://vcg.isti.cnr.it; Pisa, Italy.

Vitale S., Isaia R. (2014) - *Fractures and faults in volcanic rocks (Campi Flegrei, southern Italy): insight into volcano-tectonic processes*. International Journal of Earth Sciences, 103 (3): 801-819. doi: http://dx.doi.org/10.1007/s00531-013-0979-0.